Available online at www.sciencedirect.com
ScienceDirect
Thermochimica Acta 450 (2006) 102–104
thermochimica acta
www.elsevier.com/locate/tca

# Synthesis and thermodynamic properties of a metal-organic framework: $[LaCu_6(\mu\text{-}OH)_3(Gly)_6im_6](ClO_4)_6$

Xue-Chuan Lv [a], Zhi-Cheng Tan [a,*], Xiao-Han Gao [b], Zhi-Heng Zhang [a], Li-Ni Yang [a], Jun-Ning Zhao [a], Li-Xian Sun [a], Tao Zhang [a]

[a] *Thermochemistry Laboratory, Dalian Institute of Chemical Physics, Chinese Academy of Science, Dalian 116023, China*
[b] *State Key Laboratory of Catalysis, Dalian Institute of Chemical Physics, Chinese Academy of Science, Dalian 116023, China*

Available online 6 September 2006

**Abstract**

A metal-organic complex, which has the potential property of absorbing gases, $[LaCu_6(\mu\text{-}OH)_3(Gly)_6im_6](ClO_4)_6$ was synthesized through the self-assembly of $La^{3+}$, $Cu^{2+}$, glycine (Gly) and imidazole (Im) in aqueous solution and characterized by IR, element analysis and powder XRD. The molar heat capacity, $C_{p,m}$, was measured from $T = 80$ to 390 K with an automated adiabatic calorimeter. The thermodynamic functions $[H_T - H_{298.15}]$ and $[S_T - S_{298.15}]$ were derived from the heat capacity data with temperature interval of 5 K. The thermal stability of the complex was investigated by differential scanning calorimetry (DSC).


*Keywords:* $[LaCu_6(\mu\text{-}OH)_3(Gly)_6im_6](ClO_4)_6$; Metal-organic frameworks; Adiabatic calorimetry; Heat capacity; Thermal analysis

## 1. Introduction

Metal-organic frameworks are crystalline solids that are assembled by the connection of metal ions or clusters through molecular bridges. Since 1990s, increased attention is being focused on metal-organic frameworks (MOFs) as candidates for hydrogen storage materials. Thermodynamic properties are important to hydrogen storage materials, because temperature effects on their properties of gas storage and thermal stability decides the application of this kind of materials.

Up to date, nearly 5000 2D and 3D MOFs structures have been reported in the literature, but only a fraction of them have been examined for their porosity and far fewer of them have been studied for their thermodynamic properties. Up to now, many different ligands with carboxyl and aromatic backbones [1–3], such as phenylene, naphthalene, and biphenylene, have been used to synthesis the MOFs. In this work, using glycine (Gly) with carboxyl and amido and imidazole (Im) with nitrogen heterocyclic backbones as the organic linkers, a metal-organic complex $[LaCu_6(\mu\text{-}OH)_3(Gly)_6im_6](ClO_4)_6$, with structure of heptanuclear trigonal prismatic polyhedra, was synthesized and characterized. The heat capacities of the complex from 80 to 390 K were measured by a precision automatic calorimeter and the thermodynamic functions $[H_T - H_{298.15}]$ and $[S_T - S_{298.15}]$ were calculated with a temperature interval of 5 K.

## 2. Experimental

### 2.1. Synthesis and characterization of the complex

#### 2.1.1. Synthesis

$[LaCu_6(\mu\text{-}OH)_3(Gly)_6im_6](ClO_4)_6$ was synthesized referring to the procedure reported in literature [4]. The starting materials were analytical reagents from the Beijing Chemical Raeagent Co. Rare earth oxide ($La_2O_3$) and copper oxide (CuO) dissolved in an excess amount of perchloric acid, respectively, and the concentration of the solution was determined by EDTA titration analysis. Then, solid glycine was added to the solution of $La^{3+}$and $Cu^{2+}$ in molar ratio of $La^{3+}$:$Cu^{2+}$:Gly = 1:6:6. After the pH value of the reaction mixture was carefully adjusted to about 6.0 by slow addition of NaOH solution, imidazole was added. The solution was filtered to remove the precipitate after a further 2 h of stirring and placed in a desiccator filled with

* Corresponding author. Fax: +86 411 84691570.
*E-mail address:* tzc@dicp.ac.cn (Z.-C. Tan).

0040-6031/$ – see front matter © 2006 Elsevier B.V. All rights reserved.
doi:10.1016/j.tca.2006.07.025

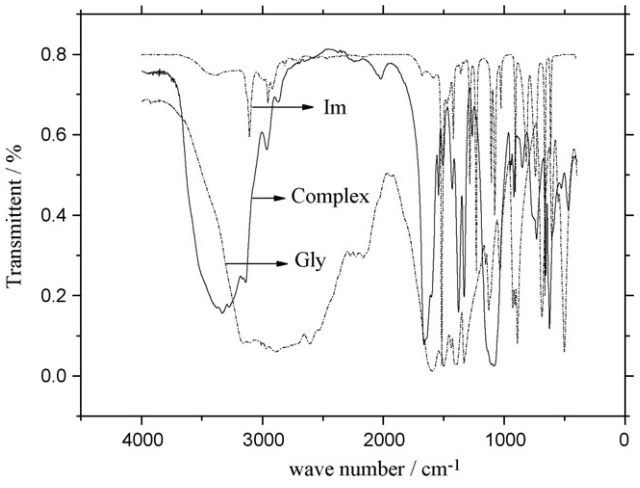


Fig. 1. The FTIR spectrum of complex and the coordination agent (glycine and imidazole).

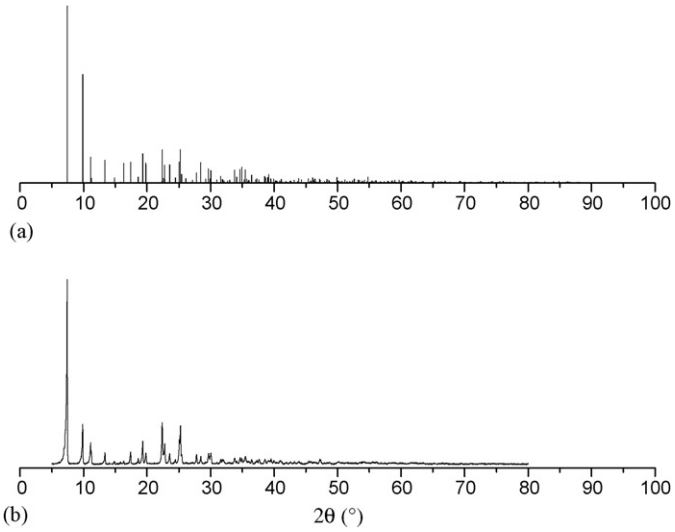


Fig. 2. Simulated powder X-ray diffraction patterns (a) for the single crystal based on the data from the documents [4] and the experiment powder X-ray diffraction patterns for the synthesis samples (b).

phosphorus pentaoxide. Blue crystals were obtained about a month later. The yields range from 30 to 35%.

### 2.1.2. Element analysis

Analyses of C, H, and N were performed on a PE-2400 Series CHNS/O Analyzer. Found: C, 17.71%; H, 2.32%; N, 12.65%, which is close to the theoretical value, C, 17.83%, H, 2.54%, N, 12.48%, Calc. for $C_{30}H_{51}Cl_6Cu_6LaN_{18}O_{39}$. The molecular formular was determined to be $[LaCu_6(\mu\text{-}OH)_3(Gly)_6im_6](ClO_4)_6$ according to literature [4]. The purity was found to be 99.33% obtained by the ratio of elementary analysis and theoretical calculation for carbon.

### 2.1.3. R spectra

IR spectra were measured using KBr pellets with a Tensor 27 (Bruker) spectrometer at 298 K. The IR spectra of the complex and the ligands (glycine and imidazole) were shown in Fig. 1. It can be seen from Fig. 1 that the symmetrical resonance frequencies, $\nu_s$(COO–), shifted from 1431 down to 1413 $cm^{-1}$, which suggested the carboxyl group of the Gly was coordinated to the metal ions. The complex has two symmetrical resonance frequencies, $\nu_s$(N–H), peaks at about 3334 and 3278 $cm^{-1}$, compared with 3130 and 3105 $cm^{-1}$ of the free glycinato ligand, which indicated that the amido group also coordinated to the metal ions. The spectrum also shows the wide peak symmetrical resonance frequencies, $\nu_s$(N–H), shifted from 3286 to 3425 down to 3166–3098 $cm^{-1}$, which is evidence of the coordination of imidazole molecules to the $Cu^{2+}$ ions.

### 2.1.4. Powder XRD

The structure and phase purity of the complex were characterized by powder XRD (Rigaku D/max-2500, 50 kV, 200 mA) with Cu Kα radiation. X-ray diffractometer. Program-Diamond-Crystal and Molecular Structure Visualization, Version 3.1 was used to transform the single crystalline data to the powder XRD patterns shown in Fig. 2(a). The experimental powder XRD patterns are shown in Fig. 2(b). Comparison of Fig. 2(a) with Fig. 2(b), shows a little difference between the two patterns. So the conclusion can be drawn that the sample was the expected complex $[LaCu_6(\mu\text{-}OH)_3(Gly)_6im_6](ClO_4)_6$, and its phase purity was very high.

## 2.2. Adiabatic calorimetry

A precision automatic adiabatic calorimeter was applied to measure the heat capacity of the compound. The calorimeter was established in Thermochemistry Laboratory of Dalian Institute of Chemical Physics, Chinese Academy of Sciences. The principle and structure of the instrument have been described in detail elsewhere [5–9]. Prior to the heat capacity measurement of the sample, the molar heat capacities of α-$Al_2O_3$, the standard reference material, were measured from $T = 78$ to 400 K to verify the reliability of the calorimeter. The results showed that the deviation of our calibration data from those of NIST was within ±0.3% over the whole temperature range.

The heat capacity measurements were continuously and automatically carried out by means of the standard method of intermittently heating the sample and alternately measuring the temperature. The heating rate and the temperature increments of the experimental points were generally controlled at (0.1–0.4 K $min^{-1}$) and (1–4 K). The heating duration was 10 min and the temperature drift rates of the sample cell measured in an equilibrium period were always kept within $10^{-3}$ to $10^{-4}$ K $min^{-1}$ during the acquisition of all heat-capacity data.

The mass of $[LaCu_6(\mu\text{-}OH)_3(Gly)_6im_6](ClO_4)_6$ used for the measurement was 1.6909 g, which was equivalent to 0.000836 mol based on the molar mass $M = 2020.74$ g $mol^{-1}$.

## 2.3. DSC

Thermal analysis of $[LaCu_6(\mu\text{-}OH)_3(Gly)_6im_6](ClO_4)_6$ was performed with a DSC-141 (SETARAM, France) at 10 K $min^{-1}$ under nitrogen at 50 mL $min^{-1}$. The mass of the sample was

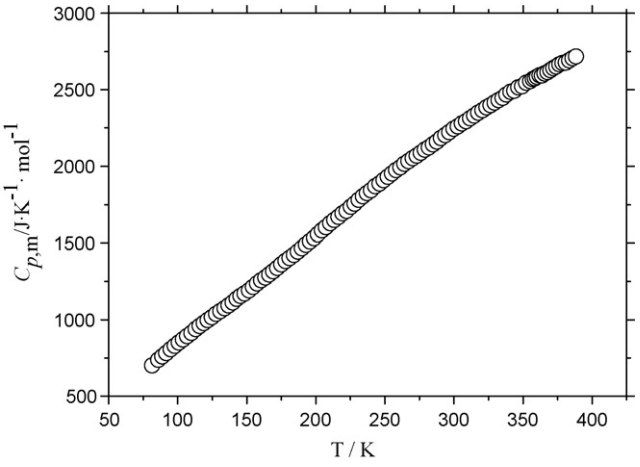


Fig. 3. Experimental molar heat capacity plotted against temperature of the complex.

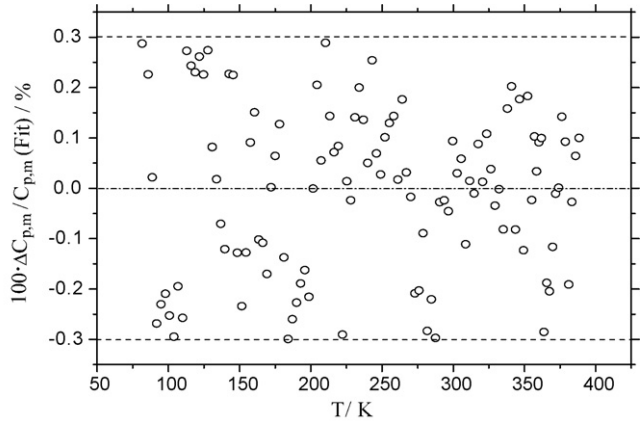


Fig. 4. The plot of relative deviations of the experimental heat capacity values of the sample, $C_{p,m}$(Expt), from the fitting heat-capacity values, $C_{p,m}$(Fit), vs. the absolute temperature ($T$) [$\Delta C_{p,m} = C_{p,m}(\text{Expt}) - C_{p,m}(\text{Fit})$].

2.3 mg. The experiment was conducted down to 160 K, cooled by liquid nitrogen.

## 3. Results and discussion

### 3.1. Molar heat capacity and thermodynamic functions

The experimental molar heat capacities, $C_{p,m}$, and temperature, $T$, from $T = 80$ K to 390 K of $[LaCu_6(\mu\text{-}OH)_3(Gly)_6im_6](ClO_4)_6$ are presented in Table 1 (see supplementary data) and plotted in Fig. 3. The heat capacity curve was continuous and smooth. A polynomial equation was obtained by least square fitting.

From $T = 80$ to 390 K:

$$C_{p,m}\,(\text{J K mol}^{-1}) = 1806.4 + 1133.8x - 165.97x^2 - 228.29x^3 + 224.82x^4 + 112.76x^5 - 162.68x^6 \quad (1)$$

where $x$ is the reduced temperature, $x = [T(\text{K}) - 235]/155$ and $R^2$ is 0.9999.

The relative deviation of the smoothed heat capacities from those obtained from the experiment versus the temperature is plotted in Fig. 4. The relative deviations were all within ±0.3%, which was within the calibration of the instrument.

The thermodynamic functions $[H_T - H_{298.15}]$ and $[S_T - S_{298.15}]$ of the compound were calculated in the temperature range from $T = 80$ to 390 K with a temperature interval of 5 K in terms of the polynomials of heat capacity and the thermodynamic relationship and listed in Table 2 (see supplementary data).

### 3.2. DSC analysis

The DSC curve from 160 to 670 K showed the complex was stable below 470 K. From 575 K, an exothermic peak occurred due to decomposition.

## Acknowledgement

This work was financially supported by the National Natural Science Foundation of China under the grant NSFC no. 20373072.

## Appendix A. Supplementary data

Supplementary data associated with this article can be found, in the online version, at doi:10.1016/j.tca.2006.07.025.

## References

[1] B. Chen, M. Eddaoudi, S.T. Hyde, M. O'Keeffe, O.M. Yaghi, Science 291 (2001) 1021–1023.
[2] J.L.C. Rowsell, A.R. Millward, K.S. Park, O.M. Yaghi, J. Am. Chem. Soc. 126 (2004) 5666.
[3] N.L. Rosi, J. Eckert, M. Eddaoudi, D.T. Vodak, J. Kim, M. O3Keeffe, O.M. Yaghi, Science 300 (2003) 1127.
[4] W.-X. Du, J.-J. Zhang, S.-M. Hu, et al., J. Mol. Struct. 701 (2004) 25–30.
[5] Z.C. Tan, J.B. Zhang, S.H. Meng, A low-temperature automated adiabatic calorimeter, J. Therm. Anal. Cal. 55 (1999) 283–289.
[6] M.H. Wang, Z.C. Tan, X.H. Sun, H.T. Zhang, B.P. Liu, L.X. Sun, T. Zhang, J. Chem. Eng. Data 50 (2005) 270–273.
[7] Z.C. Tan, G.Y. Sun, Y. Sun, et al., J. Therm. Anal. 45 (1995) 59–67.
[8] Z.C. Tan, G.Y. Sun, Y.J. Song, L. Wang, J.R. Han, Y.S. Liu, et al., Thermochim. Acta 252–253 (2000) 247–253.
[9] Z.C. Tan, L.X. Sun, S.H. Meng, L. Li, P. Yu, B.P. Liu, J.B. Zhang, J. Chem. Thermodyn. 34 (2002) 1417–1429.